ELSEVIER

Journal of Hazardous Materials B132 (2006) 196–201

Journal of Hazardous Materials

www.elsevier.com/locate/jhazmat

Photo-Fenton discoloration of the azo dye X-3B over pillared bentonites containing iron

Yimin Li *, Yueqing Lu, Xiaoliu Zhu

Department of Chemistry, Shaoxing University, Zhejiang Shaoxing 312000, PR China

Received 14 March 2005; received in revised form 29 July 2005; accepted 30 July 2005

Abstract

Both Fe pillared bentonite (Fe-B) and Al-Fe pillared bentonite (Al/Fe-B) were prepared and used as heterogeneous catalysts for the photo-Fenton discoloration of azo dye X-3B under UV irradiation. The catalysts were characterized by XRD, BET and TEM. The effects of solution pH, H_2O_2 concentration, dye concentration and catalyst loading on the rate of discoloration were investigated in detail. The results indicate that the Fe-B and Al/Fe-B have high BET surface area (114.6 and 194.2 m^2/g, respectively). Both the heterogeneous photo-Fenton processes employing the Fe-B or the Al/Fe-B as catalyst exhibit higher photo-catalytic activity compared to their corresponding homogeneous photo-Fenton process. The amount of Fe ions leached from the Al/Fe-B into the solution is much lower than that leached from the Fe-B during the reaction process.

Keywords: Fe pillared bentonite; Al-Fe pillared bentonite; Photo-Fenton; Reactive brilliant red X-3B; Long-term stability

1. Introduction

Fenton and photo-Fenton processes are considered as most promising for the remediation of wastewaters containing a variety of toxic substances [1–5]. The processes involve the generation of highly reactive hydroxyl radical ($^{\bullet}OH$), which can oxidize and mineralize almost all the organic molecules owing to its high oxidation potential ($E^{\circ} = +2.8$ V) [6]. However, Fenton and photo-Fenton processes in homogeneous media require the removal of the sludge containing Fe ions after wastewater treatment, which is expensive in labor, reagents and time [7,8]. This drawback can be overcome by using supported Fenton catalysts. Various supports used in heterogeneous photo-Fenton reactions have been reported, such as zeolites [8,9], Nafion film or Nafion pellet [10,11], polytheylene copylymers [12] and silica fabrics [7,13]. Deactivation of some heterogeneous catalysts is often observed owing to Fe-ion leached from the catalysts during photo-Fenton reaction. Therefore, it is a very important issue to develop a heterogeneous Fenton catalyst with higher catalytic activity and long-term stability at reasonable cost.

Pillared clay (PILC) represents a new class of microporous materials that have potential for the use as catalysts due to their unique properties and structures as well as low cost [14,15]. Wastewater treatment by catalytic wet oxidation using H_2O_2 (CWPO) and pillared clays containing iron as heterogeneous catalysts has been widely investigated [16,17]. Compared with pillared clays containing Fe, mixed metal oxide pillared clays (e.g. Al-Fe, Fe-Cr) usually exhibit enhanced surface area, surface acidity [18] and more satisfaction results for organic compounds total oxidant in water during CWPO [19,20].

In the present work, both Fe pillared bentonite (Fe-B) and Al-Fe pillared bentonite (Al/Fe-B) were prepared and tested as heterogeneous catalysts for the photo-Fenton discoloration of azo dye X-3B. The photo-catalytic activity employing the heterogeneous catalysts is compared with their corresponding homogeneous Fenton reagents at the same experimental conditions. Effects of parameters like solution pH, H_2O_2 concentration, catalyst loading and initial X-3B concentration on the rate of discoloration were studied in detail. In addition, the structural characteristics of the catalysts were also examined by using XRD, BET and TEM.

2. Experimental

2.1. Materials

The used bentonite was primarily Na^+-montmorillonite from Mongolia Automony, China. The cation exchange capacity

* Corresponding author. Tel.: +86 575 8341526; fax: +86 575 8342380.
E-mail address: liymj@mail.sxptt.zj.cn (Y. Li).

0304-3894/$ – see front matter © 2006 Published by Elsevier B.V.
doi:10.1016/j.jhazmat.2005.07.090

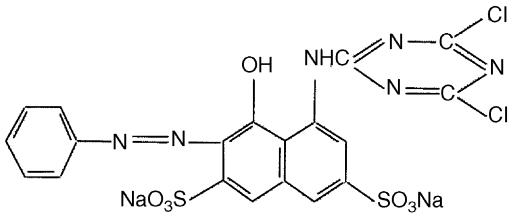

Fig. 1. Chemical structure of X-3B.

(CEC) of the bentonite is 105 meq per 100 g. Analytical grade of H_2O_2 (30%, w/v), $Fe(NO_3)_3{\cdot}9H_2O$, $AlCl_3{\cdot}6H_2O$, $FeCl_3{\cdot}6H_2O$, NaOH and Na_2CO_3 were purchased from Shanghai chemicals. The dye of Reactive brilliant red X-3B (98%) was purchased from Jining dye manufacture of Shandong, China, and used directly without further purification. The chemical structure of X-3B is shown in Fig. 1.

2.2. Catalysts preparation

Fe pillared bentonite was prepared by a procedure reported by Feng et al. [21], after some modifications. Na_2CO_3 solution was added dropwise to a vigorously stirred solution of iron nitrate until the Na^+/Fe^{3+} molar ratio was equal to 2, and the concentration of $[Fe^{3+}]$ was equal to 0.2 mol l^{-1}. After aging for 2 days at room temperature, the solution was slowly added into 2 wt.% aqueous suspension of the bentonite under stirring. The final Fe/clay ratio was equal to 2 mol kg^{-1} of dry clay. The suspension was stirred for additional 2 h and aged 2 days at 373 K in an autoclave. The precipitate was separated by centrifuging and washed several times with deionized water, and then dried at 353 K. The dried solid was ground to 100 mesh and calcined at 673 K for 3 h. The obtained sample was as Fe-B.

Al/Fe pillared bentonite was prepared according to reported by Guo and Al-Dahhan [17]. NaOH solution was slowly added to the mixed solution containing 0.18 mol l^{-1} $AlCl_3$ and 0.02 mol l^{-1} $FeCl_3$ at 353 K until the OH/(Al + Fe) molar ratio was equal to 1.9. The obtained solution was aged 2 days at room temperature, and added dropwise to the 2 wt.% aqueous suspension of the bentonite under stirring. The final (Al + Fe)/clay ratio was equal to 10 mol kg^{-1} of dry clay. The suspension was stirred for additional 2 h and aged 1 day at room temperature, then separated by centrifuging and washed until total elimination of chloride ions. After drying at 353 K, the dried solid then was ground to 100 mesh. Finally, the powder was calcined at 673 K for 3 h, while the obtained sample was labeled Al/Fe-B.

2.3. Characterization of catalysts

The X-ray diffraction (XRD) patterns of the catalysts were measured with a D/Max-III powder diffractometer equipped with Cu Kα radiation, BET surface areas were obtained by measuring the adsorption–desorption isotherms of N_2 at 77 K using a Coutter Omnisorp 100 apparatus. JEOL/JEM-1011 transmission electron microscope was used for the TEM images of the catalysts.

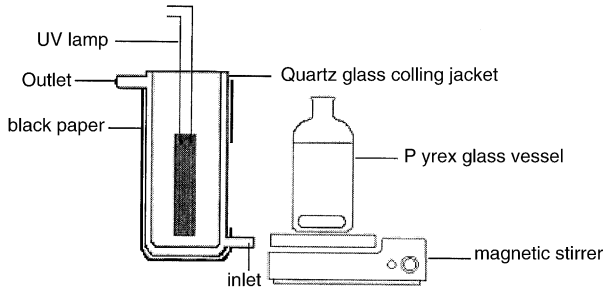

Fig. 2. Schematic diagram of the experimental setup.

2.4. Photochemical experiments

The schematic diagram of the experimental setup is shown in Fig. 2. Irradiation source was a 125 W Hg lamp (365 nm, Shanghai Yarning lamp factory) equipped with a quartz glass cooling jacket with water circulation. In typical experiment, a solution of 100 ml containing 10^{-4} mol l^{-1} X-3B and the Al/F-B or Fe-B catalyst was held in a Pyrex glass vessel, the pH of X-3B solution was adjusted to desired values with HCl and NaOH solution, and the temperature was maintained at 25 °C. Prior to irradiation, the suspension was magnetically stirred in the dark condition for 30 min to establish the adsorption–desorption equilibrium between the catalyst and X-3B. H_2O_2 was added to the reaction solution at the beginning of the irradiation. Throughout the experiment, the suspension was stirred to ensure a good dispersion of the catalyst. At a given irradiation time intervals (e.g. 0, 10, 20, 30 min, . . .), 3 ml aliquots were sampled, filtered through a membrane of pore size 0.45 μm and then analyzed with a 722 spectrophototneter (Shanghai Analytical Instrument Factory).

2.5. Analytical methods

The X-3B concentration was determined by its absorbance at 536 nm. The content of iron in the catalysts and the amount of Fe ions leached from catalysts into the solution was determined by AAS (Beijing Second Optical Instrument Factory, WFX-1F2B2). Chemical oxygen demand (COD) was measured according to the standard methods for water and wastewater [22].

3. Results and discussion

3.1. Characterization results of catalysts

Table 1 gives the d_{001} spacing, BET surface area and percentage of α-Fe_2O_3 for each sample. Compared with the original

Table 1
Physico-chemical characterization of the samples

Sample	d_{001} (nm)	S_{BET} (m^2/g)	Fe_2O_3 (wt.%)
Original bentonite	1.259	31.8	2.64
Al/Fe-B	1.879	194.2	15.3
Fe-B	1.761	114.6	15.9

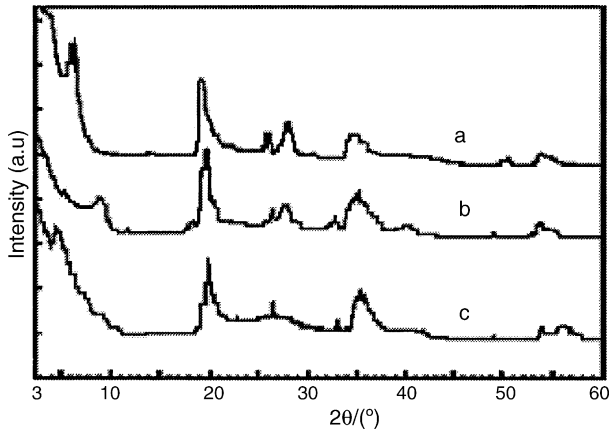

Fig. 3. XRD patterns of the samples (a) original bentonite, (b) Fe-Al-B and (c)Al/Fe-B.

bentonite, both the pillared bentonites exhibit much higher d_{001} spacing and BET surface area, especially in the Al/Fe-B. The mass percentage of α-Fe_2O_3 in the Al/Fe-B is nearly as same as that in the Fe-B.

In the XRD patterns of the Al/Fe-B and the Fe-B (Fig. 3), the diffraction peaks at $2\theta = 33.2°$, 35.7° and 54.0° are attributed to the α-Fe_2O_3(hematite) crystallite. The TEM images of the Al/Fe-B and the Fe-B display the particle of Fe_2O_3 was about 5 nm.

3.2. X-3B discoloration by heterogeneous and homogeneous processes

Fig. 4 shows the degradation of X-3B in the dark and under UV light irradiation with Fe-B or Al/Fe-B catalyst, and the degradation of X-3B in corresponding homogeneous photo-Fenton processes. With H_2O_2 and Fe-B or Al/Fe-B but in the dark (curve a and curve b), the decrease of X-3B concentration is 4% and 6.7%, respectively. The result is mainly attributed

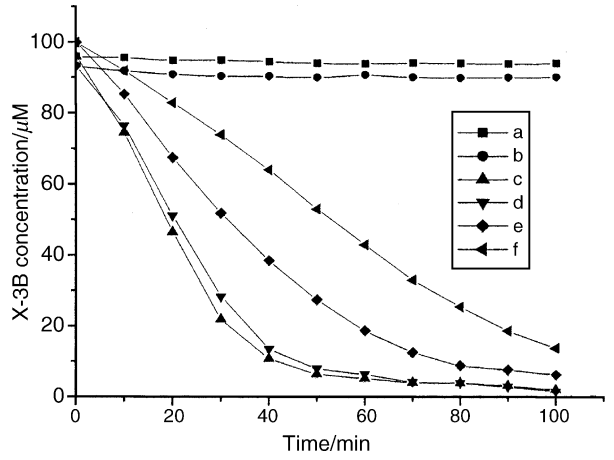

Fig. 4. Comparison between the heterogeneous photo-Fenton processes with corresponding homogeneous photo-Fenton process ($[X\text{-}3B] = 10^{-4}$ mol l^{-1}; $[H_2O_2] = 10^{-2}$ mol l^{-1}; pH 3.0) (a) in the dark but with 0.5 g l^{-1} Fe-B; (b) in the dark but with 0.5 g l^{-1} Al/Fe-B; (c) with 0.5 g l^{-1} Fe-B and UV; (d) with 0.5 g l^{-1} Al/Fe-B and UV; (e) with 0.65 mg l^{-1} Fe^{3+} and UV; (f) with 0.18 mg l^{-1} Fe^{3+} and UV.

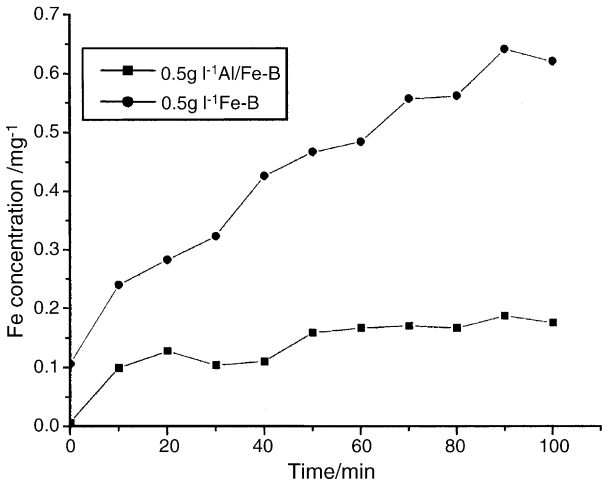

Fig. 5. Fe concentration in solution as a function of time $[X\text{-}3B] = 10^{-4}$ mol l^{-1}; $[H_2O_2] = 10^{-2}$ mol l^{-1}; pH 3.0; UV light.

to the adsorption of the dye on the catalyst surface, and also matches very well with higher BET surface area on the Al/Fe-B. In the presence of H_2O_2 and UV light, the X-3B degradation processes over the Fe-B and the Al/Fe-B were presented in curve c and curve d, which are quite fast and efficient processes, and the percent of X-3B discoloration are all over than 98% after 100 min, whereas the removal of COD are about 68%.

In order to evaluate the extent of the homogeneous photo-Fenton process leading to the discoloration of X-3B in the heterogeneous catalysis by Al/Fe-B or Fe-B, we examined the Fe ions concentration in the solution as a function of reaction time by AAS, and the results are depicted in Fig. 5 (the final pH is 3.09 in both the reaction systems). The highest concentration of total Fe ions leached from the Al/Fe-B and Fe-B is, respectively, 0.18 and 0.65 mg l^{-1}. According to an estimation of the highest Fe ions concentration, the amount of Fe ions leached is 0.33% and 1.1% of the total iron content in the Al/Fe-B and Fe-B, respectively. The lower Fe ions leached from the Al/Fe-B is due to the existence of a strong interaction between iron and aluminum pillared [17,20]. The results also indicate that the long-term stability of the Al/Fe-B catalyst is superior to that of the Fe-B in the photo-Fenton processes. The discolorations of X-3B in both the homogeneous photo-Fenton processes with 0.18 or 0.65 mg l^{-1} Fe^{3+} concentration are displayed in curve e and curve f, respectively. The comparison of the results in the heterogeneous photo-Fenton and the corresponding homogeneous photo-Fenton processes (curves c and e, curves d and f), illustrates obviously that the discoloration rates of X-3B in the heterogeneous photo-Fenton are faster than that of the homogeneous photo-Fenton processes. The fact originates from two aspects: one is the oxidation by OH radicals that come from the catalysis by the heterogeneous catalysts, and the other is the oxidation by OH radicals formed in the homogeneous photo-Fenton process [23]. But the contribution of homogeneous photo-Fenton catalysis to the overall discoloration of X-3B in heterogeneous photo-catalysis is limited. Furthermore, compared with the catalysis process on the Fe-B, the contribution coming from homogeneous photo-Fenton process for the total discoloration of X-3B on the Al/Fe-B

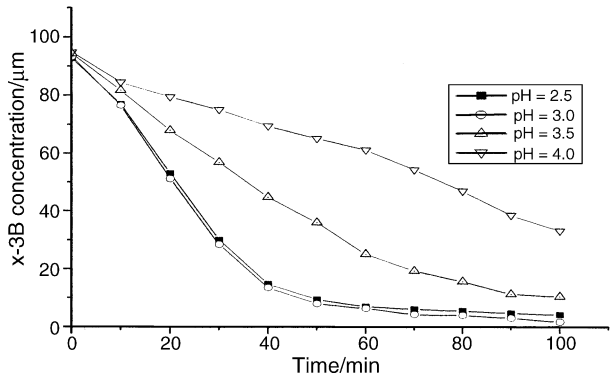

Fig. 6. Effect of pH on the discoloration of X-3B under UV irradiation [X-3B] = 10^{-4} mol l^{-1}; [H_2O_2] = 10^{-2} mol l^{-1}; 0.5 g l^{-1} Al/Fe-B.

catalyst is less. Since the photo-assisted degradation of the dye occurs predominantly on the photo-catalyst surface [24], the Al/Fe-B having higher BET surface area, surface acidity and adsorption capacity should exhibit better heterogeneous contribution than the Fe-B during the photo-Fenton process. Hence, Al/Fe-B was selected to be model catalyst for overall studied process.

3.3. Effect of the experimental condition

3.3.1. Effect of pH

Fig. 6 shows the discoloration ratio of X-3B as a function of the reaction time when aqueous solution pH is varied. The optimal pH was found to be 3.0. The result is quite in agreement with the homogeneous and heterogeneous photo-Fenton process that has been observed for the discoloration of several organic compounds [25].

3.3.2. Effect of H_2O_2 concentration

The effect of initial H_2O_2 on the discoloration of X-3B is illustrated in Fig. 7. In the presence of Al/Fe-B and UV without H_2O_2, the decrease of X-3B concentration is very limited except that the dye is adsorbed on the Al/Fe-B catalyst surface. As the H_2O_2 concentration increase from 1.0×10^{-3} to 1.0×10^{-2} mol l^{-1}, the discoloration of X-3B is also increased. But the discoloration of X-3B slows slightly down beyond 1.0×10^{-2} mol l^{-1}. The fact is due to the increase hydroxyl radical concentration as the addition of H_2O_2, but at higher H_2O_2 concentration, the decrease in discoloration is due to the hydroxyl radical scavenging effect of H_2O_2 (Eqs. (1) and (2)) and recombination of hydroxyl radicals (Eq. (3)) [26].

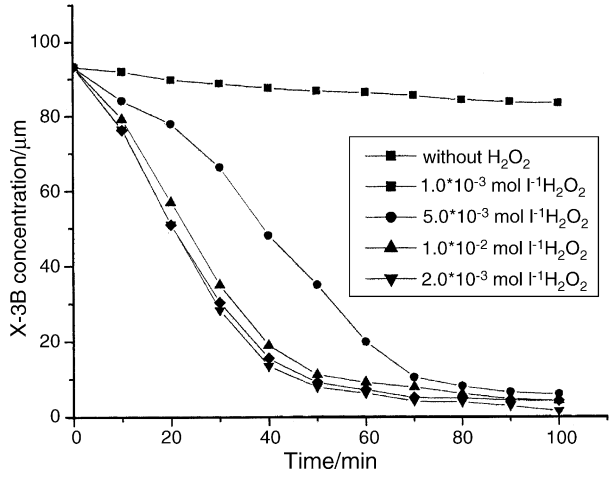

Fig. 7. Effect of H_2O_2 concentration on the discoloration of X-3B under UV irradiation [X-3B] = 10^{-4} mol l^{-1}; pH 3.0; 0.5 g l^{-1} Al/Fe-B.

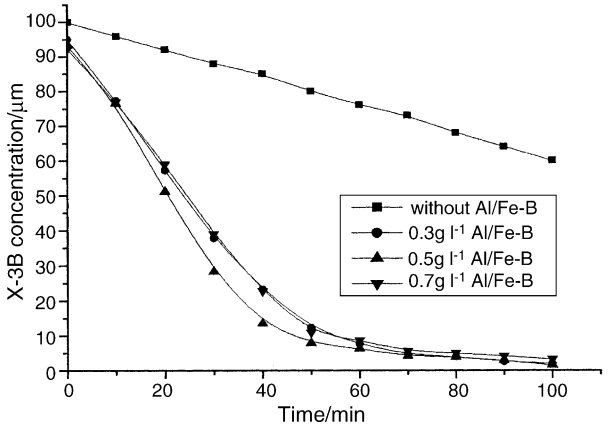

Fig. 8. Effect of Al/Fe-B dosage on the discoloration of X-3B under UV irradiation [X-3B] = 10^{-4} mol l^{-1}; pH 3.0; [H_2O_2] = 10^{-2} mol l^{-1}.

$$H_2O_2 + {}^{\bullet}OH \rightarrow H_2O + HO_2{}^{\bullet} \quad (1)$$

$$HO_2{}^{\bullet} + {}^{\bullet}OH \rightarrow H_2O + O_2 \quad (2)$$

$${}^{\bullet}OH + {}^{\bullet}OH \rightarrow H_2O_2 \quad (3)$$

3.3.3. Effect of the Al/Fe-B catalyst loading

The effect of Al/Fe-B catalyst loading on the discoloration of X-3B is shown in Fig. 8. In the presence of UV and H_2O_2 without Al/Fe-B, the discoloration ratio of X-3B reaches about 40% in 100 min owing to the oxidation of X-3B by $^{\bullet}OH$ radical from the direct photolysis of H_2O_2 under UV irradiation. The discoloration ratio of X-3B increases with the catalyst loading up to 0.5 g l^{-1}, and decreases when the catalyst loading is larger than 0.5 g l^{-1}. This phenomenon is in agreement with the case observed typically in heterogeneous photo-catalysis reaction [24,27]. The increase of the Al/Fe-B catalyst loading will increase the amount of Fe ions involved in the photo-Fenton process, which in turn, increase the number of hydroxyl radical, but the solution will become more turbid as the catalyst dosage increases, which will decrease the penetration of UV light and the number of hydroxyl radical.

3.3.4. Effect of initial X-3B concentration

Fig. 9 depicts the effect of initial X-3B concentration on its discoloration. The result clearly reveals that the increase of X-3B concentration will decrease its discoloration. The results correspond to those from literature [24]. As X-3B concentration increases, the absorption of UV light by X-3B solution also significantly increases. As a result, the number of photons penetrating solution is decreased, and the hydroxyl radical concentration lowered. Whereas, it should be noted that even at a high initial

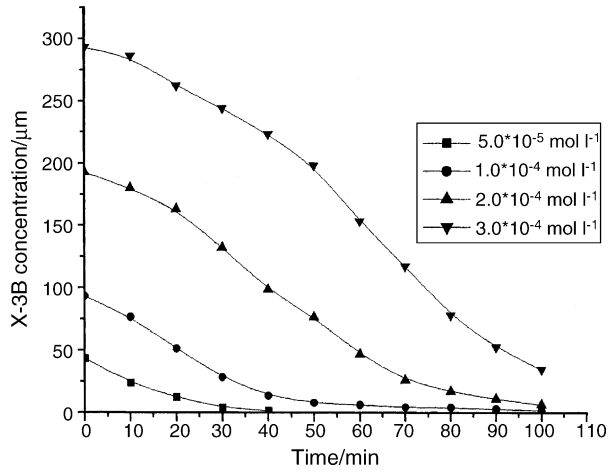

Fig. 9. Effect of the initial concentration of X-3B on the discoloration ratio under UV irradiation $[H_2O_2] = 10^{-2}$ mol l^{-1}; pH 3.0; 0.5 g l^{-1} Al/Fe-B.

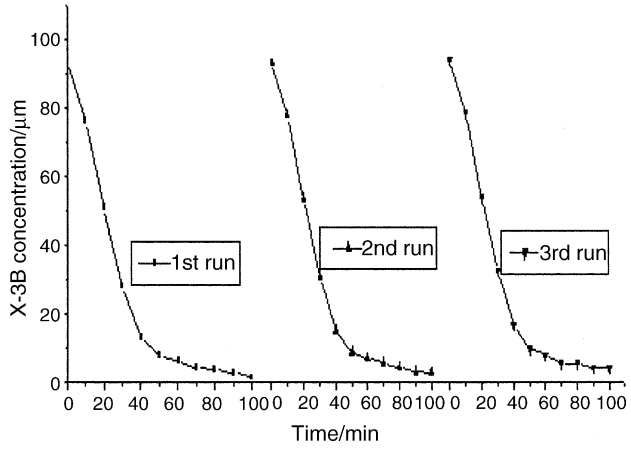

Fig. 10. Repetitive discoloration ratio of X-3B under UV irradiation [X-3B] = 10^{-4} mol l^{-1}; $[H_2O_2] = 10^{-2}$ mol l^{-1}; pH 3.0; 0.5 g l^{-1} Al/Fe-B.

concentration of X-3B, for example, 3×10^{-4} mol l^{-1}, the discoloration ratio can also be achieved about 88% after 100 min.

3.4. Recycling of the Al/Fe-B catalyst

Fig. 10 shows the discoloration nature of X-3B on the Al/Fe-B in three consecutive photo-Fenton experiments. After each experiment, the catalyst was separated from the solution by filtration, washed with deionized water, and then X-3B and H_2O_2 were added before the next experiment. It is clearly seen that the Al/Fe-B catalyst has an ideal long-term stability, as the photocatalysis activity is not significant difference during these three reactions. This result also coincides with the low Fe ions leached from the Al/Fe-B presented in Fig. 5.

4. Conclusion

Both Fe pillared bentonite (Fe-B) and Al-Fe pillared bentonite (Al/Fe-B) were used as heterogeneous photo-Fenton catalysts for the discoloration of azo dye X-3B. The results show that both the heterogeneous photo-Fenton catalysis employed Fe-B or Al/Fe-B as catalyst exhibit higher photo-catalytic activity compared to their corresponding homogeneous photo-Fenton process. Complete discoloration of the dye solution can be carried out in the heterogeneous photo-Fenton processes at the optimal condition. The amount of Fe ions leached from the Al/Fe-B into the solution is much lower than that leached from the Fe-B during reaction process even though the photo-catalytic activity is not significant difference between Al/Fe-B and Fe-B. In addition, the Al/Fe-B catalyst is easily recovered and regenerated, and it also possesses excellent long-term stability.

Acknowledgements

This work was supported by the Natural Science Foundation of Zhejiang province (202018). One of the authors (Li, Y.-M.) would like to thank Dr. Liu, Y. and Dr. Wen, L.-H. for their helpful discussions.

References

[1] M.R. Hoffmann, S.T. Martin, W. Choi, D.W. Bahnemann, Environmental applications of semiconductor photocatalysis, Chem. Rev. 95 (1995) 69–96.
[2] F.J. Benitez, J. Beltran-Heredia, J.L. Acero, F.J. Rubio, Oxidation of several chlorophenolic derivatives by UV irradiation and hydroxyl radicals, J. Chem. Technol. Biotechnol. 76 (2001) 312–320.
[3] E. Chamarro, A. Marco, S. Esplugas, Use of Fenton reagent to improve organic chemical biodegrality, Water Res. 35 (2001) 1047–1051.
[4] E.R. Bandala, D. Martinez, E. Martinezc, D.D. Dionysiou, Degradation of microcystin-LR toxin by Fenton and photo-Fenton processes, Toxicon. 43 (2004) 829–832.
[5] Y. Sun, J.J. Pignatello, Photochemical-reactions involved in the total mineralization of 2,4-D by Fe^{3+}/H_2O_2/UV, Environ. Sci. Technol. 27 (1993) 304–310.
[6] O. Legrini, E. Oliveros, A.M. Braun, Photochemical processes for water treatment, Chem. Rev. 93 (1993) 671–698.
[7] D. Li, T. Yuranova, P. Albers, J. Kiwi, Accelerated photobleaching of Orange II on novel ($H_5FeW_{12}O_{40}10H_2O$)/silica structured fabrics, Water Res. 38 (2004) 3541–3550.
[8] M. Rios-Enriquez, N. Shahin, C. Duran-de-Bazua, J. Lang, E. Oliveros, S.H. Bassmann, A.M. Braun, Optimization of the heterogeneous Fenton-oxidation of the model pollutant 2,4-xylidine using the optimal experimental design methodology, Solar Energy 77 (2004) 491–501.
[9] S.H. Bossmann, E. Oliveros, S. Gob, M. Kantor, A. Goppert, L. Lei, P.L. Yue, A.M. Braun, Degradation of polyvinyl alcohol (PVA) by homogeneous and heterogeneous photo catalysis applied to the photochemicaly enhanced Fenton reactions, Water Sci. Technol. 44 (2001) 257–262.
[10] J. Fernandez, J. Bandara, A. Lopez, P. Buffat, J. Kiwi, Photoassisted Fenton degradation of nonbiodegradable azo dye (Orange II) in Fe-free solutions mediated by cation transfer membranes, Langmuir 15 (1999) 185–192.
[11] J. Fernandez, J. Bandara, A. Lopez, P. Alberz, J. Kiwi, Efficient photo-assisted Fenton catalysis mediated by Fe ions on Nafion membranes active in the abatement of nonbiodegradable azo-dye, Chem. Commun. (1998) 1493–1494.
[12] M.R. Dhananjeyan, E. Mielzcarski, K.R. Thampi, P. Buffat, M. Bensimon, A. Kulik, J. Mielcarski, J. Kiwi, Photodynamics and surface characterization of TiO_2 and Fe_2O_3 photocatalysts immobilized on modified polyethylene films, J. Phys. Chem. B 105 (2001) 12046–12055.
[13] A. Bozz, T. Yuranova, E. Mielzcarski, J. Mielzcarski, P.A. Buffat, P. Lais, J. Kiwi, Superior biodegradability mediated by immobilized Fe-fabrics of waste waters compared to Fenton homogeneous reactions, Appl. Catal. B: Environ. 42 (2003) 289–303.

[14] C. Ooka, H. Yoshida, M. Horio, K. Suzuki, T. Hattori, Adsorptive and photocatalytic performance of TiO_2 pillared montmorillonite in degradation of endocrine disruptors having different hydrophobicity, Appl. Catal. B: Environ. 41 (2003) 313–321.
[15] K-I. Shimizu, T. Kaneko, T. Fujishima, T. Kodama, H. Yoshida, Y. Kitayama, Selective oxidation of liquid hydrocarbons over photoirradiated TiO_2 pillared clays, Appl. Catal. A: Gen. 225 (2002) 185–191.
[16] E. Guelou, J. Barrault, J. Fournier, J.-M. Tatibouet, Active iron species in the catalytic wet peroxide oxidation of phenol over pillared clays containing iron, Appl. Catal. B: Environ. 44 (2003) 1–8.
[17] J. Guo, M. Al-Dahhan, Catalytic wet oxidation of phenol by hydrogen peroxide over pillared clay catalyst, Ind. Eng. Chem. Res. 42 (2003) 2450–2460.
[18] T. Mishra, K. Parida, Transition metal oxide pillared clay: 5. Synthesis, characterization and catalytic activity of iron-chromium mixed oxide pillared montmorillonite, Appl. Catal. A: Gen. 174 (1998) 91–98.
[19] J. Barrault, M. Abdellaoui, C. Bouchoule, A. Majeste, T.M. Tatibouet, A. Louloudi, N. Papayannakos, N.H. Gangas, Catalytic wet peroxide oxidation over mixed (Al-Fe) pillared clays, Appl. Catal. B: Environ. 27 (2000) L225–L230.
[20] J. Chirchi, A. Ghorbel, Use of various Fe-modifled montmorillonite samples for 4-nitrophenol degradation by H_2O_2, Appl. Clay Sci. 21 (2002) 271–276.
[21] J. Feng, X. Hu, P.L. Yue, H.Y. Zhu, G.Q. Lu, A novel laponite clay-based Fe nanocomposite and its photo-catalytic activity in photo-assisted degradation of Orange-II, Chem. Eng. Sci. 58 (2003) 679–685.
[22] A.E. Greenberg, R.R. Trusell, L.S. Clesceri (Eds.), Standard Methods for the Examination of Water and Wastewater, 17th ed., American Public Health Association, Washington, DC, 1989.
[23] J. Feng, X. Hu, P.L. Yue, H.Y. Zhu, G.Q. Lu, Discoloration and mineralization of Reactive Red HE-3B by heterogeneous photo-Fenton reaction, Water Res. 37 (2003) 3776–3784.
[24] S. Chakrabarti, B.K. Dutta, Photocatalytic degradation of model texile dyes in wastewater using ZnO as semiconductor catalyst, J. Hazard. Mater. B 112 (2004) 269–278.
[25] S. Parra, V. Nadtotechenko, P. Albers, J. Kiwi, Discoloration of azo-dyes at biocompatible pH-values through an Fe-histidine complex immobilized on Nafion via Fenton-like processes, J. Phys. Chem. B 108 (2004) 4439–4448.
[26] C. Walling, Fenton's reagent, Acc. Chem. Res. 8 (1975) 125–131.
[27] I. Bouzaida, C. Ferronato, J.M. Chovelon, M.E. Rammahb, J.M. Herrmann, Heterogeneous photocatalytic degradation of the anthraquinonic dye, Acid Blue 25 (AB25): a kinetic approach, J. Photochem. photobiol. A: Chem. 168 (2004) 23–30.